

Storage of water on vegetation under simulated rainfall of varying intensity

R.F. Keim ^{a,*}, A.E. Skaugset ^b, M. Weiler ^c

^a School of Renewable Natural Resources, Louisiana State University, LSU AgCenter, 227 Renewable Natural Resources Building, Baton Rouge, LA 70803, USA

^b Department of Forest Engineering, Oregon State University, 215 Peavy Hall, Corvallis, OR 97331, USA

^c Faculty of Forestry, University of British Columbia, 2424 Main Mall, Vancouver, BC, Canada V6T1Z4

Received 6 December 2004; received in revised form 19 July 2005; accepted 25 July 2005

Available online 13 October 2005

Abstract

Little is understood about how storage of water on forest canopies varies during rainfall, even though storage changes intensity of throughfall and thus affects a variety of hydrological processes. In this study, laboratory rainfall simulation experiments using varying intensities yielded a better understanding of dynamics of rainfall storage on woody vegetation. Branches of eight species generally retained more water at higher rainfall intensities than at lower intensities, but incremental storage gains decreased as rainfall intensity increased. Leaf area was the best predictor of storage, especially for broadleaved species. Stored water ranged from 0.05 to 1.1 mm effective depth on leaves, depending on species and rainfall intensity. Storage was generally about 0.2 mm greater at rainfall intensity 420 mm h⁻¹ than at 20 mm h⁻¹. Needle-leaved branches generally retained more water per leaf area than did branches from broadleaved species, but branches that stored most at lower rainfall intensities tended to accumulate less additional storage at higher intensities. A simple nonlinear model was capable of predicting both magnitude (good model performance) and temporal scale (fair model performance) of storage responses to varying rainfall intensities. We hypothesize a conceptual mechanical model of canopy storage during rainfall that includes the concepts of static and dynamic storage to account for intensity-driven changes in storage. Scaling up observations to the canopy scale using LAI resulted in an estimate of canopy storage that generally agrees with estimates by traditional methods.

© 2005 Elsevier Ltd. All rights reserved.

Keywords: Canopy storage; Rainfall simulation; Canopy interception; Throughfall; Rainfall intensity; Forest canopy

1. Introduction

Detention of water on vegetation is the basic process controlling interactions of precipitation with plant canopies. Water temporarily stored on canopy surfaces is readily evaporated and is therefore an important component of the hydrological cycle in most regions. In addition, temporary storage of rainfall incident on canopies smooths rainfall intensities and reduces maxi-

imum rainfall rates in throughfall compared to rainfall [65,34].

Canopy storage is difficult to measure in the field. Several researchers [52,12,5,6] have estimated canopy storage of entire stands by measuring their attenuation of electromagnetic waves, Hancock and Crowther [22] calculated storage on standing trees by measuring deflections of branches under load from stored water, while Lundberg [44] and Storck et al. [61] measured canopy storage of snow by weighing entire trees.

All of these methods are expensive and impractical for many applications, so researchers and practitioners most often estimate canopy storage indirectly. The running

* Corresponding author. Tel./fax: +1 225 578 4169.
E-mail address: rkeim@lsu.edu (R.F. Keim).

difference between rainfall and the sum of throughfall and evaporation has sometimes served as an estimate of storage during storms [47,69], but the most common approach remains estimating canopy storage “capacity” from storm-total precipitation by the method of Leyton et al. [40]. This method results in a simple estimate of water available for evaporation by disregarding details of the rainfall-storage–drip process.

Despite the general success of the canopy storage capacity concept as the basis of estimating evaporation from intercepted water, results of direct [12,35] and indirect [34] field investigations have confirmed assumptions of the Rutter et al. [58] model and laboratory findings by Aston [1] that storage increases with rainfall intensity. Because these storage changes are the mechanism of intensity smoothing, a better understanding is required for a process-based model of intensity smoothing by canopies. The scarcity of data means models have so far been limited to black-box approaches at the canopy scale [34]. Ultimately, a physically-based understanding of canopy storage responses to rainfall would allow mechanistic modeling of throughfall at fine temporal and spatial scales. Whelan and Anderson [68] and Davie and Durocher [16,17] have demonstrated the potential of such models for predicting evaporation, but did not consider intensity effects.

An alternative to measuring or estimating storage in large, complex forest canopies in varying meteorological conditions is to measure storage on smaller units of canopy under simulated rainfall in a controlled environment. Most previous experiments of this type have generally been designed to estimate parameters required by the widely-used canopy interception evaporation model of Rutter et al. [58]: either canopy storage [28, 31,15,62], or storage-dependent drainage rates [23,55, 56]. There has been only limited work with simulated rainfall to quantify canopy storage and drainage in response to rainfall of varying characteristics, most notably Aston [1], who measured storage and drip on tree seedlings of varying leaf area under several rainfall intensities, and Calder et al. [13], who measured storage in tree branches under simulated rainfall of varying drop sizes and intensities. However, both of those experiments applied simulated rainfall of temporally constant intensity, and there have been no published experimental observations of storage responses to temporally varying rainfall intensities.

The objective of this research is to quantify storage of precipitation on vegetation in response to varying rainfall intensities. First, we will describe the storage responses to varying rainfall intensities of branches from several species of trees and shrubs of varying morphology. Second, we will generalize and quantify canopy storage responses to varying rainfall intensities and the resulting smoothing effect on throughfall intensities by modeling vegetation as a reservoir for precipitation.

Finally, we will estimate canopy-scale storage during rainfall rates typical of field conditions by scaling up branch-scale observations.

2. Methods

2.1. Vegetation samples

We collected vegetation samples up to 2 m length by cutting branches from eight different species of shrubs and trees common to the Pacific Northwest region of the USA. We selected five broadleaved species [*Acer macrophyllum* (bigleaf maple), *Alnus rubra* (red alder), *Rubus spectabilis* (salmonberry), *Rubus parviflorus* (thimbleberry), and *Acer circinatum* (vine maple)] and three needle-leaved species [*Pseudotsuga menziesii* ssp. *menziesii* (Douglas-fir), *Tsuga heterophylla* (western hemlock), and *Thuja plicata* (western redcedar)] (nomenclature follows [57]). *A. macrophyllum*, *A. rubra*, *P. menziesii*, *T. heterophylla*, and *T. plicata* are overstory trees, and *R. spectabilis*, *R. parviflorus*, and *A. circinatum* are woody shrubs. Each sample underwent rainfall simulation less than six hours after collection, and we sealed the cut end of each sample in paraffin to prevent wilting during this time. We collected samples and conducted tests on broadleaved species during August and September of 2002, and needle-leaved species from January to June of 2003.

Subsequent measurements of the samples resulted in three ways to characterize each sample: biomass of sample, biomass of leaves/branchlets, and (one-sided, projected) leaf area (LA). After rainfall simulation, we disassembled each sample into leaves and stems (for broadleaved species) or branchlets and stems (for needle-leaved species), arranged the resulting parts without overlap in a frame, and took vertical-view digital photographs of the frame and vegetation for measurement of surface area. Finally, we obtained the dry biomass of leaves/branchlets and stems by weighing samples oven dried at 65 °C for at least 24 h.

Analysis of the digital photographs of disassembled samples entailed using VegMeasurement software (D. Johnson, Oregon State University Department of Rangeland Resources) to classify each pixel of images as either leaf or not leaf, using a qualitatively calibrated filter to discriminate greenness or brightness, and calculate LA as the proportion of the image classified as leaves multiplied by the total area of the image. We used the definition of LA as one-sided, projected leaf area to approximate leaf surface area exposed to rainfall. This approximation may have been more accurate for the broadleaved species than it was for needle-leaved species, which are more round in cross section. Therefore, we also estimated LA for needle-leaved samples using published allometric relationships between total surface

area of the needle-leaved species and projected LA [2,3] and biomass [54,32], but these methods resulted in widely varying estimates of total surface area. In addition, surfaces of broad leaves are not flat. For example, hairs on leaf surfaces are also likely to affect storage, but are not easily measured. Therefore, we adopted projected LA as measured in the photographs as the standard for all species. Analysis of stem surface area was the same as analysis of leaf area, but applying a correction to projected area to estimate total surface area assuming cylindrical cross section: surface area = $\pi \cdot$ (projected area).

2.2. Rainfall simulation and data collection

We constructed a rainfall simulator in the laboratory that consisted of individually controllable nozzles employable singly or in groups to simulate four intensi-

ties of rainfall (Fig. 1). The spray rig consisted of a manifold under constant pressure feeding five separate spray nozzles. Each spray nozzle was mounted on the end of a valve stub pipe from the manifold, so it could be activated independently of the other nozzles. Each valve was controlled by an electrical solenoid (similar to the design of Miller [48]) wired to a wall switch at the rainfall simulator control panel. This design allowed changing of intensity in about 2 s. Water supply and pressure was by filtered municipal water supply in combination with a pressure regulator to maintain 1.4 bar (20 psi) at the nozzles. Pressure gauges between each solenoid valve and spray nozzle allowed monitoring of pressure at each nozzle independently, so that head losses in the system did not affect calibration. The spray rig was 4.9 m above the ground (~ 4 m above the vegetation sample).

Four different combinations of one or more nozzles allowed simulation of four rainfall intensities: 20, 60, 250 and 420 mm h⁻¹ (Table 1). These intensities simulate moderate to very heavy rain, so that evaporation from samples was small compared to rainfall and drip rates. The mean drop sizes produced by each nozzle or combination of nozzles (according to specifications published by Spraying Systems Co., Wheaton, Illinois, USA) approximately matched those of natural rainfall (Table 1), although the range of drop sizes was likely less in spray than in natural rainfall. Calibration was by test simulations into continuous 0.25-m² pans placed in a grid on the floor beneath the spray. The coefficient of variation of water accumulated in these pans was 0.2–0.4 (depending on intensity) in the middle 2.25 m² of the sample area where the vegetation samples were placed.

We suspended vegetation specimens on a 5-mm cable attached to an electronic balance (Mettler-Toledo SR32001) mounted on the ceiling above the spray rig (Fig. 1). A computer controlled the balance and recorded the raw weight of the sample at 10 Hz during spraying. Adjustable cross-member cables on the suspension cable allowed each branch to be suspended at the same orientation as it was growing in the field. This position was maintained throughout the test, so that mechanical responses of the branches to simulated rainfall did not exactly duplicate the natural situation.

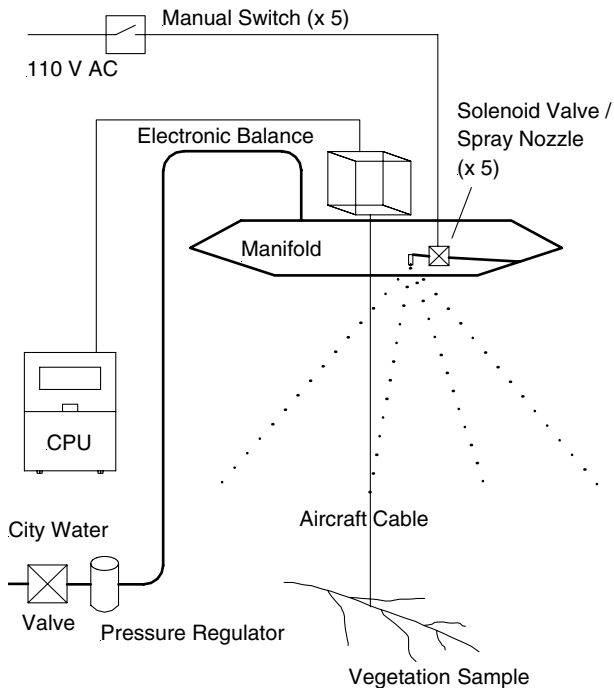


Fig. 1. Diagram of the experimental apparatus for simulating rainfall and measuring water stored on sample branches.

Table 1
Rainfall intensities and mean drop diameters produced by the rainfall simulator

Mean rainfall intensity (mm h ⁻¹)	Nozzles ^a	Mean drop size (mm)	Expected mean drop size range (mm) ^b
20	1 × G3.5 (1.60 mm)	1.0	1.1–2.2
60	2 × G6.5 (2.39 mm)	1.3	1.5–2.6
250	G3.5 + 2 × G6.5 + G25 (9.55 mm)	2.5	2.0–3.4
420	G3.5 + 2 × G6.5 + 2 × G25	2.8	2.3–3.7

^a Model numbers for nozzles produced by Spraying Systems, Inc. (Wheaton, Illinois, USA).

^b Range of values reported by Laws and Parsons [37], Best [4], and Mason and Andrews [45].

Each test began with simulated rainfall at the lowest intensity (20 mm h^{-1}), and continued until weight of the sample reached a quasi-steady value (S_{steady}). We then increased the rainfall intensity to 60 mm h^{-1} , waited for the weight to stabilize, and repeated the sequence for intensities of 250 and 420 mm h^{-1} . When the weight stabilized at the 420 mm h^{-1} intensity, we turned off the simulator and continued weighing the sample until drip rates dropped substantially ($\sim 3\text{--}5 \text{ min}$) and we judged evaporative losses may have been a large enough proportion of the weight loss to confound estimation of drip rates.

There were two corrections to the raw weight data required for measurement of water stored during simulated rain. First, we subtracted from the raw data the time-varying weight of water detained on the suspension cable, obtained by running tests with no vegetation sample. Second, we subtracted the apparent weight from the force of water drops impinging on the specimen and suspension cable. Mass accumulating on branches requires that force be exerted on the branch, caused by momentum of the falling drops being transferred to the branch [21]. This force varied by rainfall intensity and by vegetation specimen because the orientation of vegetative surfaces to rainfall and flexibility of the vegetation varied. It was therefore necessary to estimate the force of raindrops on every sample for each intensity. We accomplished this by analyzing the response of the apparent sample weight to 10-s interruptions in spray while the sample was at steady-state storage. For each sample and intensity, we estimated the force as the instantaneous apparent additional weight caused by the onset of simulated rainfall at the end of the 10-s interruption, averaged over four repetitions. The force of raindrops accounted for less than 5% of the total apparent weight of all samples, but water stored on the suspension cable accounted for up to 17% of the apparent weight for samples that were very light.

2.3. Analysis of rainfall-storage–drainage relationships

Drainage (D ; [dimensions L^3T^{-1}]) from a linear reservoir is linearly proportional to storage (S [L^3]):

$$D(t) = kS(t), \quad (1)$$

where k [T^{-1}] is a constant of proportionality. In canopy storage, the analysis is customarily one-dimensional, so the dimensions of D become [LT^{-1}], and the dimensions of S become [L].

The equation of mass conservation for water in the canopy, including rainfall (R ; [LT^{-1}]), storage, and drip, is

$$R(t) - D(t) = \frac{dS}{dt}. \quad (2)$$

In Eq. (2), D subsumes stemflow and evaporation; in our experiments stemflow could not occur and we ignored evaporation as low compared to R and D . Substituting Eq. (1) into Eq. (2) gives the governing equation for mass conservation in a canopy where drip is proportional to storage:

$$R(t) - kS(t) = \frac{dS}{dt}. \quad (3)$$

Solving Eq. (3) with constant R and initial condition $S(0) = 0$ gives

$$S(t) = \frac{R}{k}(1 - e^{-kt}). \quad (4)$$

The limit of Eq. (4) as $t \rightarrow \infty$ gives

$$S_{\infty} = \frac{R}{k}, \quad (5)$$

which is the storage when steady inflow and outflow approach equilibrium and storage approaches steady state (S_{∞}) [14]. Eq. (4) describes canopy storage approaching S_{∞} asymptotically from a dry canopy at the onset of rainfall. This relationship has a long history of application in canopy interception research [39,46], but its implication for canopy storage during rainfall of varying intensities has not been fully explored.

Linear reservoirs have the property that storage is linearly related to (steady) rainfall intensities by Eq. (5). However, the only published data on intensity-dependent storage suggests that incremental gain in steady-state storage decrease with rainfall intensity [1]. Also, Calder [8] found linear drainage (Eq. (3)) did not fit experimentally determined recession rates of storage ($R = 0$ and $S(0) > 0$), and most other research in canopy interception has also assumed or experimentally found some form of nonlinearity in the storage–drainage relationship (see review by Keim and Skaugset [34]). Therefore, we next consider the possibility that a nonlinear reservoir is a more appropriate model for canopy storage.

A simple nonlinear reservoir is

$$D(t) = bS(t)^n, \quad (6)$$

where n is a dimensionless constant of nonlinearity and b is analogous to k but with dimensions [$\text{L}^{1-n}\text{T}^{-1}$]. Although Eq. (6) is not commonly applied in canopy storage modeling, Domingo et al. [18] found it described the observed storage–drainage relationship better than the more commonly used drip equation originally assumed by Rutter et al. [58]. Substituting Eq. (6) into Eq. (2) gives the governing equation for mass conservation in a canopy where drip is related to storage by Eq. (6):

$$R(t) - bS(t)^n = \frac{dS}{dt}. \quad (7)$$

Analytical solutions to Eq. (7) are only tractable for some values of n [60]. However, it is possible to estimate k and n from data for some special cases. One such case is during steady-state rainfall at $t \rightarrow \infty$, when storage is also steady ($S = S_\infty$), $dS/dt = 0$, and Eq. (7) reduces to

$$S_\infty = cR^N, \quad (8)$$

where $N = 1/n$ [-] and $c = (1/b)^N [\text{L}^{1-N}\text{T}^N]$ [60].

To assess the viability of reservoir models (Eqs. (5) and (8)) for modeling steady-state storage under varying rainfall intensities, we approximated S_∞ with S_{steady} for each of the four intensities in the simulated rainfall tests, and then fitted parameters for the linear and nonlinear models. We calculated parameter k of the linear model (Eq. (5)) from S_{steady} and R of each intensity of all tests. We fitted parameters of the nonlinear model (Eq. (8)) by numerical searches for values of c and N that optimized fit of Eq. (8) to observed S_{steady} for each test sequence of R . The parameter searches maximized the Nash–Sutcliffe efficiency, E , as the objective function [51].

We assessed the ability of the models to predict storage responses to varying rainfall intensity by their ability to predict the time to steady-state storage, S_{steady} , after the onset of a new intensity. It was difficult to precisely estimate this time from data, however, because of noise in the measurements of sample weight and because samples sometimes slowly increased weight during “steady-state” storage (Section 3). To avoid this problem, we measured response of each sample as the time to reach storage equal to $0.8 \cdot S_{\text{steady}}$ after onset of increased intensity (T80). The variance of fractional response times is less than the variance of maximum response times when initial rates of change of responses are faster than rates of change near the maximum response, so fractional response variables are more precise estimates of response times [29].

3. Results

3.1. Storage responses to varying intensities

Leaf area (LA) was the characteristic of samples most related to steady-state water storage, especially for broadleaved species (Fig. 2a). Needle-leaved species, especially *T. heterophylla*, stored more water per LA than did broadleaved species at all intensities. Conversely, needle-leaved species stored less water per biomass than did broadleaved species, but biomass of samples was an unreliable predictor of storage across species (Fig. 2b). Species with thin leaves or thin stems (*R. spectabilis*, *R. parviflorus*, and *A. circinatum*) stored more water per biomass than species with thicker leaves or larger stems (e.g., needle-leaved species). Biomass of leaves was of intermediate value as a predictor of storage (Fig. 2c). The highest specific storage in relation to

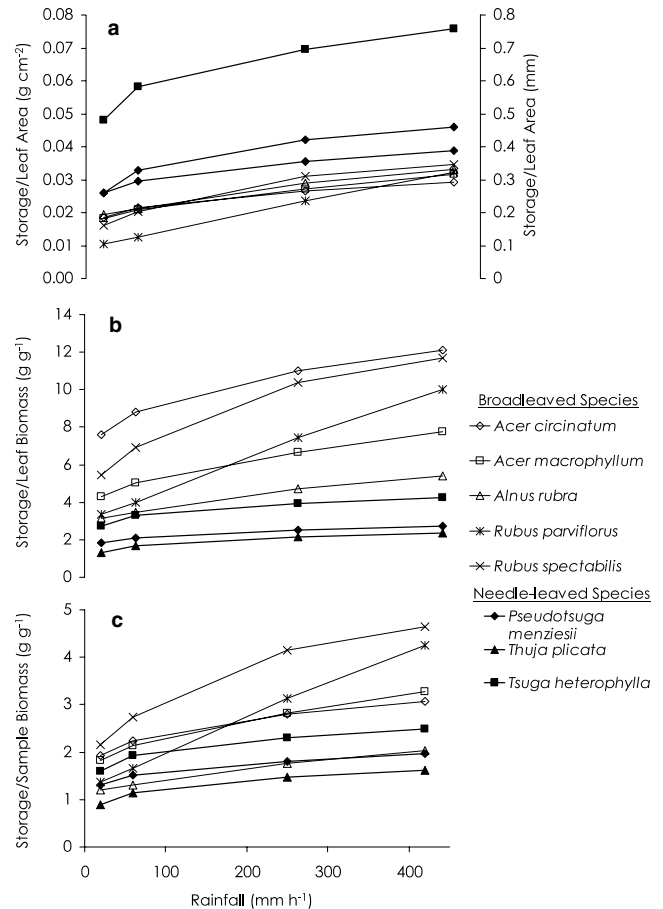


Fig. 2. Storage of water on branches under simulated rainfall, normalized to either (a) leaf area; (b) leaf biomass; or (c) total biomass of samples. Values are equilibrium storage averaged across all tests for each species ($5 \leq n \leq 10$).

leaf biomass was on the thin, rough leaves of *Rubus* spp., especially at the highest simulated rainfall intensities. The effectiveness of LA in normalizing storage among species also extended to effectiveness in normalizing among samples of the same species (not shown). Therefore, we conducted further analyses on the basis of storage (g) per LA (cm^2). Conveniently, $10 \cdot \text{storage/LA} = \text{average depth of water on leaf surfaces (mm)}$, and $\text{storage (mm)} \cdot \text{leaf area index (LAI; dimensionless)} = \text{canopy storage per LAI (mm)}$.

Steady-state storage generally increased with increased simulated rainfall intensity (Table 2, Figs. 2 and 3a). Only three of 57 samples (*A. rubra* 5, *A. rubra* 8, and *R. parviflorus* 7) stored less water at rainfall intensity 60 mm h^{-1} than at 20 mm h^{-1} , and one sample (*T. heterophylla* 6) stored less water at 250 mm h^{-1} than at 60 mm h^{-1} . All 57 samples stored more water at 420 mm h^{-1} than at 250 mm h^{-1} (Table 2).

The typical response of most species and samples to the onset of simulated rainfall at 20 mm h^{-1} was for water stored on branches to come to equilibrium within 5–10 min, with equilibrium storage reached much more

Table 2
Sample branches subjected to simulated rainfall

Sample	Position in canopy ^a	Dry weight (g)		Leaf area (m ²)	Steady-state storage (g) at intensity (mm h ⁻¹)			
		Branch	Leaves only		20	60	250	420
<i>Acer macrophyllum</i> (bigleaf maple)								
1	L	49.2	18.9	0.56	67	95	139	201
2	L	86.7	41.6	0.63	141	157	181	206
3	L	38.3	20.3	0.51	106	125	160	170
4	L	82.0	27.9	0.89	183	191	220	237
5	L	66.8	29.2	0.63	134	136	175	188
6	L	99.1	42.7	0.83	165	191	243	279
7	L	62.7	25.2	0.79	74	106	184	225
<i>Alnus rubra</i> (red alder)								
1	L	67.5	15.1	0.31	54	68	103	121
2	M	41.3	20.5	0.25	34	37	67	76
3	L	39.2	16.2	0.30	54	56	79	94
4	L	59.9	17.6	0.34	94	99	110	123
5	L	28.2	11.8	0.22	59	57	69	75
6	L	91.2	42.0	0.56	81	99	160	190
7	L	37.5	11.5	0.23	40	47	62	81
8	M	123.2	60.7	0.70	184	182	199	207
9	U	80.6	36.7	0.60	80	88	118	135
10	M	60.3	25.3	0.29	54	66	109	122
<i>Rubus spectabilis</i> (salmonberry)								
1	S	28.2	12.7	0.54	50	66	122	148
2	S	14.6	6.5	0.25	29	45	58	69
3	S	25.1	10.1	0.42	85	109	144	155
4	S	14.9	6.4	0.25	30	37	72	86
5	S	31.3	13.9	0.44	95	116	169	179
6	S	32.5	11.6	0.47	81	94	131	150
7	S	57.2	22.6	0.67	162	173	214	231
8	S	27.6	11.3	0.21	26	33	74	75
9	S	22.9	8.7	0.15	25	35	62	69
10	S	11.4	3.4	0.17	24	32	46	52
<i>Rubus parviflorus</i> (thimbleberry)								
1	S	28.2	13.8	0.40	46	59	120	153
2	S	25.1	11.8	0.38	30	39	88	120
3	S	17.5	7.7	0.26	30	34	58	81
4	S	14.2	4.7	0.19	32	39	63	77
5	S	38.4	16.8	0.35	24	36	71	114
6	S	24.9	12.0	0.32	19	24	57	85
7	S	24.5	9.4	0.30	35	34	57	76
<i>Acer circinatum</i> (vine maple)								
1	S	62.5	14.7	0.63	118	150	183	193
2	S	32.7	9.1	0.37	80	81	93	99
3	S	32.5	8.1	0.40	71	82	110	119
4	S	76.2	16.3	0.63	102	123	165	190
5	S	82.4	25.6	0.96	145	185	237	270
6	S	61.2	15.1	0.57	123	133	158	176
<i>Pseudotsuga menziesii</i> ssp. <i>menziesii</i> (Douglas-fir)								
1	L	134.8	88.8	1.11	253	273	295	323
2	L	260.0	193.9	1.33	360	415	525	570
3	U	208.5	118.2	0.44	161	181	223	248
4	L	132.7	110.6	0.94	186	203	261	284
5	U	128.1	83.4	0.44	132	145	172	190
6	L	109.7	87.8	0.83	157	209	241	259
<i>Tsuga heterophylla</i> (western hemlock)								
1	L	141.6	120.8	0.30	165	217	289	323
2	U	54.9	37.2	0.16	71	87	109	119
3	L	108.7	52.8	0.48	223	263	314	323
4	L	32.3	14.1	0.13	68	87	104	116

(continued on next page)

Table 2 (continued)

Sample	Position in canopy ^a	Dry weight (g)		Leaf area (m ²)	Steady-state storage (g) at intensity (mm h ⁻¹)			
		Branch	Leaves only		20	60	250	420
5	L	85.8	66.6	0.29	114	134	156	170
6	L	54.3	40.2	0.19	92	100	99	105
<i>Thuja plicata</i> (western redcedar)								
1	L	196.3	127.1	0.75	191	243	323	354
2	L	146.1	113.4	0.64	109	153	200	223
3	M	108.2	83.6	0.23	76	90	116	127
4	M	48.6	33.5	0.23	59	74	97	104
5	L	217.3	127.1	0.64	182	232	282	305

^a L = lower, M = middle, U = upper canopy; S = shrub layer.

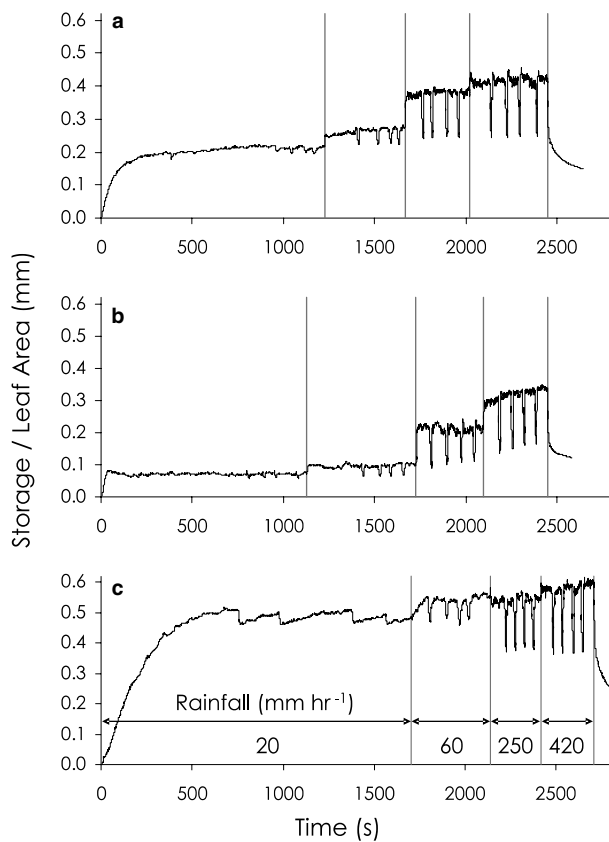


Fig. 3. Example data from tests of rainfall simulation on branches. In each case, the black line is the depth-equivalent mass of water stored on a branch, thin vertical lines indicate step increases in rainfall intensity (shown in panel c). Dips in stored water are the result of 10-s interruptions in sprinkling. Data are (a) *R. spectabilis* sample 5; (b) *R. parviflorus* sample 5; (c) and *T. heterophylla* sample 6.

quickly after the onset of successively higher intensities (Fig. 3a). However, there were several atypical but repeated behaviors worthy of note. Nineteen of the 57 samples continued slow increases in storage throughout at least one intensity (Fig. 3b). For later analyses based on steady-state storage for samples that showed this behavior, we used the maximum storage near the end of the test. Starting from an initially dry condition, most

samples accumulated storage monotonically until reaching equilibrium, but eight of the 57 samples reached an early peak in storage followed by lower equilibrium storage (Fig. 3b). The minimum storage reached during successive 10-s interruptions in spraying increased or remained constant with increasing rainfall intensity for all but 16 of the 57 samples (Fig. 3c). The final common atypical behavior was slow accumulation of storage (Fig. 3c); variance of response times is discussed in Section 3.2.

3.2. Modeling storage responses to varying intensities

Estimates of the linear reservoir parameter k from (5) varied by species and simulated rainfall intensity (Fig. 4). Differences by species are the result of varying equilibrium storage (Fig. 2). Differences in the estimate of k by intensity, however, show that the linear model cannot adequately describe the rainfall-storage-drip relationship for the sample branches. This lack of fit is also evident in plots of storage as a function of rainfall

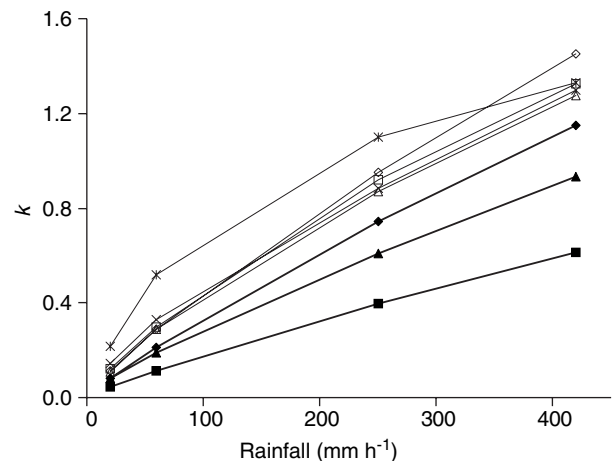


Fig. 4. Constant of proportionality, k , of a linear reservoir model describing water stored on branches, estimated from equilibrium storage and intensity of simulated rainfall for each of eight species (see key in Fig. 2). Values are normalized by one-sided sample leaf area and averaged across all samples for each species.

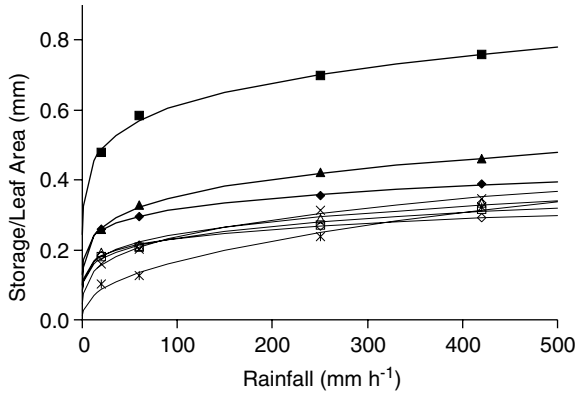


Fig. 5. Nonlinear models of water stored on branches of several species at rainfall-intensity-dependent equilibrium, fitted to data averaged across all tests per species (see key in Fig. 2).

intensity (Fig. 2), which must be linear and pass through the origin for proper fit of a linear model.

The nonlinear model (Eq. (8)) fit observations of intensity-dependent storage well (Fig. 5). The efficiency of best-fit models predicting storage of individual samples over varying simulated rainfall intensity ranged from $E = 0.76$ to $E > 0.99$, with mean $E = 0.97$. Efficiency of the model in predicting average responses by species ranged from $E = 0.97$ to $E > 0.99$, with mean $E = 0.99$.

In addition to efficiently predicting equilibrium storage (the calibration data), the fitted nonlinear models

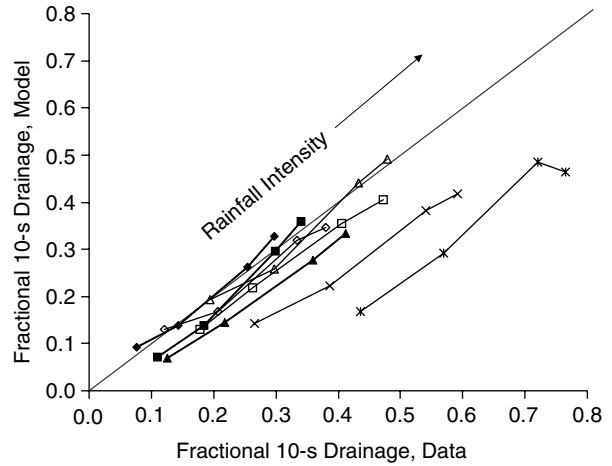


Fig. 6. Observed drainage of water stored on branches during 10-s interruptions of simulated rainfall, expressed as fractions of intensity-dependent equilibrium storage, compared to predictions of a nonlinear rainfall-storage model calibrated to equilibrium storage amounts. Observed values are averages of 1–4 interruptions per sample, and averaged across all samples for each species ($5 \leq n \leq 10$). The diagonal line indicates 1:1 agreement between data and models.

also predicted responses to varying rainfall intensity surprisingly well. The fitted models' predictions of fractional drainage in response to the 10-s interruptions in spraying matched observed values for some species, but underestimated fractional drainage from *R. spectabilis* and *R. parviflorus* (Fig. 6). The fitted models

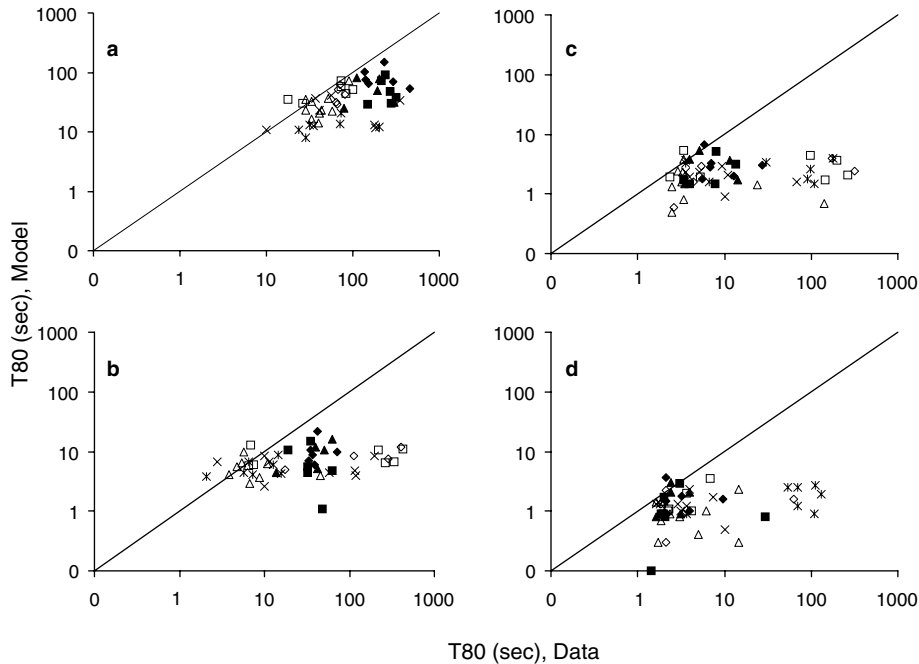


Fig. 7. Relationship between observed and modeled response times of water stored on branches to increases in intensity of simulated rainfall, quantified by the time from onset of rainfall intensity to $0.8 \cdot$ eventual equilibrium storage at the new intensity (T80). The panels are for simulated rainfall intensity steps from (a) 0 to 20 mm h^{-1} , (b) 20 to 60 mm h^{-1} , (c) 60 to 250 mm h^{-1} , and (d) 250 to 420 mm h^{-1} . Each symbol represents the response time of a single sample (see species key in Fig. 2), and lines indicate 1:1 agreement between data and models.

predicted the increases of 10-s fractional drainage with rainfall intensity well, as evidenced by the slope of unity in a plot of model vs. data (Fig. 6).

The nonlinear model underpredicted the time required for samples to come to equilibrium storage (T80) for more than 80% of samples, and there was considerably more variance in observations compared to modeled response times (Fig. 7). Variation in measured T80 was not clearly related to any variable except rainfall intensity and species; i.e., sample leaf area and biomass were not significant predictors of response time. Needle-leaved species were slower than broadleaved species to accumulate storage at the onset of sprinkling and in response to intensity increases up to 25 mm h^{-1} , but this relationship was reversed at the highest intensity (Fig. 7; Table 2). The species that was fastest to respond to all new intensities was *A. rubra*. Overall, fast response times were generally associated with smooth, broad leaves, and complex vegetative surfaces were slower to respond.

Best-fit parameters of the nonlinear model varied consistently by species and vegetation morphology, and best fits were in a distinct region of parameter space (Fig. 8). Needle-leaved species, especially *T. heterophylla*, tended to be best described by larger values of c than were the broadleaved species, which corresponds to generally higher equilibrium storage amounts per leaf area (Figs. 2 and 5). Broadleaved species characterized by low c were also characterized by higher N , which indicates more nearly linear increases in storage with intensity ($N = 1$ is a linear response). Physically, this means that branches that stored more water at lower rainfall intensities tended to accumulate proportionally less water at higher rainfall intensities (on a per-leaf-area basis); species that stored water more effectively were less sensitive to variations of intensity.

Least-squares regression between best-fit parameters of the nonlinear model from all tests yielded $c =$

$0.41e^{-6.5N}$ with $R^2 = 0.87$. However, the regression for the broadleaved species alone ($c = 0.31e^{-5.9N}$; $R^2 = 0.96$) was much better than for needle-leaved species alone ($c = 0.39e^{-4.4N}$; $R^2 = 0.24$) (Fig. 8). The consistent relationship between c and N suggests that dynamic storage on broadleaved species as a group depends on fewer variables than on needle-leaved species, perhaps because of less intraspecific morphological variability.

4. Discussion

Measurements of specific water storage in this study of 0.10–0.46 mm (up to 0.76 mm for *T. heterophylla*), depending on species and rainfall intensity (Table 2, Fig. 2), are comparable to previous direct measurements. Grah and Wilson [20] measured equilibrium water storage on *Pinus radiata* during heavy spray at 0.11 mm and on *Baccharis pilularis* at 0.25 mm. Aston [1] measured storage after 2 min of drainage from seedlings of two eucalypts, *Acacia longifolia*, and *P. radiata*, at 0.03–0.18 mm. We estimate these values correspond to about 0.12–0.36 mm during rainfall, based on drip rates measured in our study. Herwitz [27] measured equilibrium water storage on saplings of Australian rainforest species of 0.23–0.32 mm under simulated heavy rainfall.

There is a discrepancy in specific storage measured by dipping vegetation into water compared to sprinkling experiments, especially when water is blotted from foliage to simulate windy conditions. Storage measured this way is nearly an order of magnitude lower than under rainfall simulation. Using this method, Crockford and Richardson [15] measured storage at 0.017–0.028 mm for three eucalypts, Liu [42] measured storage at 0.036–0.041 mm for needle-leaved and broadleaved species, and Llorens and Gallart [43] measured storage at 0.104 mm (0.043 mm when blotted) for *Pinus sylvestris* needles.

Applying these estimates to canopy scale is possible by multiplying leaf storage (mm) by leaf area index (LAI; dimensionless). For example, results of our experiment suggest branch storage in Douglas-fir at constant rainfall intensity of 20 mm h^{-1} would be $S = cR^N = 0.23 \cdot 20^{0.13} = 0.34 \text{ mm}$. In a pure Douglas-fir forest with LAI of 7, canopy storage would be $0.34 \cdot 7 = 2.4 \text{ mm}$, ignoring storage on woody biomass. For comparison, Link et al. [38] estimated saturation storage at 3.0–4.1 mm for the Wind River Canopy Crane forest, which has LAI 6.9 in mixed needle-leaved species, including Douglas-fir [63], and a major component of woody biomass in the canopy [53]. Because the sprinkling method of branch-scale storage appears to match field estimates, it appears that the consistently lower estimates of storage obtained by the dipping method are inaccurate.

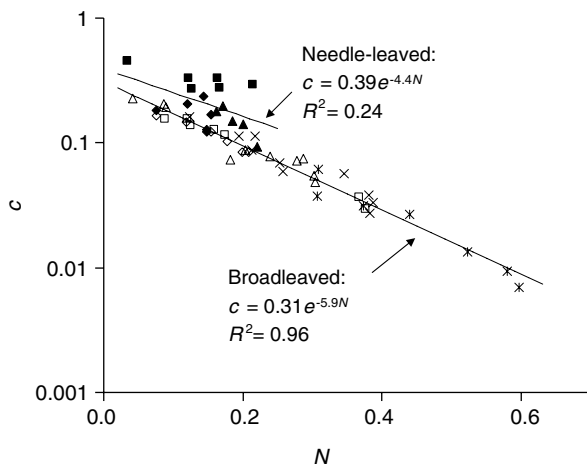


Fig. 8. Relationship between the parameters of a nonlinear model describing storage on branches as a function of simulated rainfall intensity (see species key in Fig. 2).

The poorly defined nature of canopy storage terms is a source of confusion that leads to conceptual and methodological difficulties in canopy interception research. For example, the concept of canopy storage “capacity” is common in the field, but definitions of this state vary tremendously. For example, Rutter et al. [58] and earlier workers (e.g., Leyton et al. [40]) defined storage capacity as “saturation” in terms of maximum availability for evaporation, recognizing that actual retention may exceed this value. Later modelers simplified the concept to a bucket model, defining “capacity” as a single value above which no more precipitation is retained [50]. The rationale for this simplification generally has been that water in excess of canopy saturation is not available for evaporation and need not be considered [41]. Another common definition of canopy storage capacity includes the storage amount when drip stops [26]. Confounding all these definitions are considerations of rainfall intensity and wind, which have both generally been assumed to reduce storage “capacity” [25,9,19].

Resolution of this confusion depends on adoption of a physically-based conceptual model of canopy storage. We suggest here a conceptual mechanical model of rainfall passage into, on, and through canopies. The goal is to develop a consistent nomenclature and define the processes in physical terms.

The kinetics of water detained on branches during rainfall entails static interfacial forces at the contact between water and vegetation and the atmosphere, as well as dynamic forces arising from motion of water in and impinging upon the canopy. The traditional notion of canopy storage capacity approximately coincides with the conceptual condition where the amount of water present on canopy surfaces is such that gravitational forces are balanced by interfacial and normal forces resisting movement of water, and all dynamic forces are zero. Rain falling on a canopy in this state decelerates upon impact, decreasing its momentum. This transfer of momentum has two relevant effects on water storage within the canopy. First, it adds net downward dynamic forces that work with gravity to favor drip. Canopy interception researchers have long recognized this effect. For example, Calder et al. [13] found that holding intensity approximately steady while increasing momentum of rainfall by increasing drop size results in lower storage. The second effect of rainfall transferring momentum to the canopy is to add mass of water [21], at least temporarily.

While evaporation loss from canopies depends on the reservoir of stored water in the canopy, probably largely retained by static forces (“static canopy storage”), the intensity smoothing effect of canopies depends more upon dynamic forces (“dynamic canopy storage”). Specifically, we hypothesize dynamic canopy storage (and hence intensity smoothing) to be mainly the result of

the balance between the two main effects of rain falling on wet canopies: addition of water and dislodging of existing storage. Smoothing is probably enhanced by refilling of static storage dislodged by dynamic forces external to the rainfall (i.e., wind; [30,38]), as well as by momentum transferred out of canopy water by viscous flow along vegetative surfaces [28].

An analogy for illustrating the concepts of static and dynamic storage is a porous medium. We envision “static storage capacity” as analogous to field capacity of a soil. This wetness is reached relatively quickly after rainfall ceases, and is an important characteristic of the medium. Water in excess of static storage capacity (field capacity) drains quickly, but the drainage is not instantaneous. The difference between the porous media that are soil and canopies is that water movement in soil can usually be approximated by potential flow and momentum neglected at all time scales of measurement, but momentum of water in canopies appears to be an important control on throughfall generation at short timescales.

The balance of forces and supply of mass that affects dynamic storage can conceptually result in net drainage of stored water, as assumed by many previous authors [10,11], but our experiments and the experiments of Aston [1] suggest that the more common result is net increased storage. The variability of behavior among species and within species in this study makes it difficult to infer what vegetation characteristics control the balance of forces. However, roughness of leaves seems less important than roughness of the branch as a whole. For example, species such as *R. parviflorus* with rough, broad leaves were much less effective at storing water than species with smooth leaves but complexity at the branch scale in the form of small needles as in *T. heterophylla* (Fig. 5). Other potentially important factors are leaf shape, epiphytes, and surface paniculate matter.

It is unclear why slow accumulation of storage occurred in some but not all samples in this experiment; we were unable to determine a relationship between this phenomenon and any sample characteristics except that none of the samples were of needle-leaved species. We hypothesize that slow addition of storage may have been the result of slow accumulation of water on parts of the samples not directly exposed to the simulated rainfall, either by drop splash or flow along surfaces [28].

We were also unable to determine a relationship between sample characteristics and the phenomenon of nonmonotonic accumulation of storage (Fig. 3b) except that none of the samples were of needle-leaved species. We hypothesize that the decrease from the initial maximum storage was the result of storage exceeding some threshold mass where gravity overcame surface tension in much the same way that momentum of drops moving

along surfaces can effect drainage rates that exceed rates expected by static forces alone in soils [64].

The minimum storage reached during successive 10-s interruptions in spraying increased or remained constant with increasing rainfall intensity for all but 16 of the 57 samples (e.g., Fig. 3). We infer that 10 s was too short for full drainage of dynamic canopy storage in cases where minimums increased with storage. For the samples where these minimum storage amounts were lower at higher rainfall intensity (e.g., Fig. 3c), we hypothesize that the greater momentum imparted by rainfall effected drainage below levels expected by static forces alone, as in the case of nonmonotonic approaches to equilibrium storage.

Because biomass of branches did not correlate well to rainfall storage (even within the same species), measurements of canopy biomass, while easier to obtain than surface area, are insufficient for predicting canopy-scale storage. Unfortunately, this makes it difficult to compare our data to measurements of whole-canopy storage by Hancock and Crowther [22] and Calder and Wright [12], who reported only canopy biomass. Water storage on woody components of canopies can also vary substantially by species and morphology [15], which complicates the relationship between canopy biomass and storage.

The results from this experiment agree with data presented by Aston [1], who found canopy storage filled faster at higher rainfall intensities than at lower intensities. This effectively refutes Calder's [9] hypothesis that canopy storage increases more quickly at lower intensities. Although the rainfall simulation work by Calder et al. [13] appears to support Calder's [9] hypothesis, the rainfall simulator used by Calder et al. [13] varied only drop size substantially, while rainfall intensity remained relatively constant (drop diameter 0.5 and 1.2 mm at $R = 36 \text{ mm h}^{-1}$ and drop diameter 5.2 mm at $R = 45 \text{ mm h}^{-1}$). That experiment, therefore, seems to have been most fitted to determining the simple effect of drop kinetic energy on storage.

The measurements of storage responses to rainfall intensity variations in this study are strictly only applicable to branches receiving rainfall instead of drip from branches above, because the drop size distribution of drip does not match that of rainfall [67,7,24]. Canopy drip tends to be composed of larger drops than rain, so that kinetic energy of throughfall is greater than rainfall if drops achieve sufficient velocity [49,67]. Therefore, understory branches may show less additional storage with increased intensity, and canopy-scale storage responses to varying rainfall intensity may therefore be muted compared to branch-scale responses. However, dense canopies, where drip does not fall far enough to reach terminal velocity (about 4.5 m for 1-mm drops and 9 m for 5-mm drops [36]), may act more like large branches. Also, we speculate that intense rainfall may

be more likely to initiate stemflow or cause accumulation on normally dry part of the canopy by drop splash [28]. These processes would tend to increase storage by partitioning water into slower pathways of drainage.

The nonlinear model to describe storage as a function of rainfall intensity produced generally good fits to data, and values of the parameters were interpretable and at least moderately repeated among samples of the same species and species groups. It would be possible to derive more sophisticated models, either from first principles or simply statistically to produce better fits to data where the simple model we used here was less than satisfactory. Because storage behavior was fairly predictable, gains in modeling processes at the branch scale seem likely to yield insights into storage processes at the canopy scale.

Davie and Durocher [16,17] presented a model of forest canopies that explicitly represents inflow, storage, and drainage for each cell of a pixelated canopy. Although their goals were to reproduce spatial patterns of throughfall and they represented water movement through each pixel only stochastically, it would theoretically be possible to use their framework with the results of our experiments and three-dimensional data of leaf area and species to parameterize a discrete-element model of water transfer through canopies. Difficulties may arise from processes that do not scale well between the branch scale and canopy scale. Examples include wind, stemflow, and storage in woody biomass.

5. Conclusions

The results of these rainfall simulation experiments give quantitative estimates of how storage varies by rainfall intensity, and suggests that morphological characteristics of vegetation may play a role in this process. Branches of all eight tested species generally retained more water at higher rainfall intensities than at lower intensities, but needle-leaved branches generally retained more water per leaf area than did branches from broad-leaved species. Incremental storage gains decreased as rainfall intensity increased. Leaf area was the best predictor of storage, but this relationship was stronger for broadleaved species than for needle-leaved species. Branches that stored most water at lower rainfall intensities tended to accumulate less additional storage at higher rainfall intensities. A simple nonlinear model, $S = cR^N$, was capable of predicting both magnitude (good model performance) and temporal scale (fair model performance) of storage responses to varying rainfall intensities. We hypothesize these processes are controlled by a conceptual mechanical model of canopy storage during rainfall that includes the concepts of static storage and dynamic storage to account for intensity-driven changes in storage. Scaling up observations to the

canopy scale, using published estimates of LAI of a well-studied canopy, resulted in estimates of canopy storage that generally agreed with estimates obtained by the traditional Leyton method. The simulated rainfall intensities in this research were high; more work remains to quantify intensity-dependant storage under lower intensities.

Acknowledgements

This research was supported by grant 00-34158-8978 from the US Department of Agriculture, Cooperative State Research Education and Extension Service, Centers for Wood Utilization Research. We thank Nalini Nadkarni and Bob Van Pelt for sharing their Cedar Flats research plot, and four anonymous reviewers for helpful comments.

References

- [1] Aston AR. Rainfall interception by eight small trees. *J Hydrol* 1979;42:383–96.
- [2] Barclay HJ. Conversion of total leaf area to projected leaf area in lodgepole pine and Douglas-fir. *Tree Physiol* 1998;18:185–93.
- [3] Barclay HJ, Goodman D. Conversion of total to projected leaf area index in conifers. *Can J Botany* 2000;78:447–54.
- [4] Best AC. The size distribution of raindrops. *Quart J Roy Meteor Soc* 1950;16:16–36.
- [5] Bouten W, Swart PJF, de Water E. Microwave transmission, a new tool in forest hydrological research. *J Hydrol* 1991;124:199–230.
- [6] Bouten W, Schaap MG, Aerts J, Vermetten AWM. Monitoring and modelling canopy water storage amounts in support of atmospheric deposition studies. *J Hydrol* 1996;81:305–21.
- [7] Brandt CJ. The size distribution of throughfall drops under vegetation canopies. *Catena* 1989;16:507–24.
- [8] Calder IR. A model of transpiration and interception loss from a spruce forest in Plynlimon, central Wales. *J Hydrol* 1977;33:247–65.
- [9] Calder IR. A stochastic model of rainfall interception. *J Hydrol* 1986;89:65–71.
- [10] Calder IR. Dependence of rainfall interception of drop size: 1. Development of the two-layer stochastic model. *J Hydrol* 1996;185:363–78.
- [11] Calder IR. Rainfall interception and drop size—development and calibration of the two-layer stochastic interception model. *Tree Physiol* 1996;16:727–32.
- [12] Calder IR, Wright IR. Gamma ray attenuation studies of interception from Sitka spruce: some evidence for an additional transport mechanism. *Water Resour Res* 1986;22:409–17.
- [13] Calder IR, Hall RL, Rosier PTW, Bastable HG, Prasanna K. Dependence of rainfall interception of drop size: 2. Experimental determination of the wetting functions and two-layer stochastic model parameter for five tropical tree species. *J Hydrol* 1996;185:379–88.
- [14] Chow VT. *Handbook of applied hydrology*. New York: McGraw-Hill; 1998.
- [15] Crockford RH, Richardson DP. Partitioning of rainfall in a eucalypt forest and pine plantation in southeastern Australia III: determination of the canopy storage capacity of a dry sclerophyll eucalypt forest. *Hydrol Process* 1990;4:157–67.
- [16] Davie TJA, Durocher MG. A model to consider the spatial variability of rainfall partitioning within deciduous canopy. I. Model description. *Hydrol Process* 1997;11:1509–23.
- [17] Davie TJA, Durocher MG. A model to consider the spatial variability of rainfall partitioning within deciduous canopy. II. Model parameterization and testing. *Hydrol Process* 1997;11:1525–40.
- [18] Domingo F, Sánchez G, Moro MJ, Brenner AJ, Puigdefábregas J. Measurement and modelling of rainfall interception by three semi-arid canopies. *Agric Forest Meteorol* 1998;91:275–92.
- [19] Dunkerly D. Measuring interception loss and canopy storage in dryland vegetation: a brief review and evaluation of available research strategies. *Hydrol Process* 2000;14:669–78.
- [20] Grah RF, Wilson CC. Some components of rainfall interception. *J Forest* 1944;42:890–8.
- [21] Grubin C. Mechanics of variable mass systems. *J Franklin I* 1963;276:305–12.
- [22] Hancock NH, Crowther JM. A technique for the direct measurement of water storage on a forest canopy. *J Hydrol* 1979;41:105–22.
- [23] Hall RL. Further interception studies of heather using a wet-surface weighing lysimeter system. *J Hydrol* 1985;81:193–210.
- [24] Hall RL, Calder IR. Drop size modification by forest canopies: measurements using a disdrometer. *J Geophys Res* 1993;98:18465–70.
- [25] Halldin S, Grip H, Perttu K. Model for energy exchange of a pine forest canopy. In: Halldin S, editor. *Comparison of forest water and energy exchange models*. Copenhagen: International Society for Ecological Modelling; 1979. p. 59–75.
- [26] Hashino M, Yao H, Yoshida H. Studies and evaluations on interception processes during rainfall based on a tank model. *J Hydrol* 2002;255:1–11.
- [27] Herwitz SR. Interception storage capacities of tropical rainforest canopy trees. *J Hydrol* 1986;77:237–52.
- [28] Herwitz SR. Raindrop impact and water flow on the vegetative surfaces of trees and the effects on stemflow and throughfall generation. *Earth Surf Proc Landf* 1987;12:425–32.
- [29] Hjerdt KN. Deconvoluting the hydrologic response of a small till catchment: spatial variability of groundwater level and quality in relation to streamflow. Ph.D. Dissertation, State University of New York, College of Environmental Science and Forestry, Syracuse; 2002. 204 p.
- [30] Hörmann G, Brandig A, Clemen T, Herbst M, Hinrichs A, Thamm F. Calculation and simulation of wind controlled canopy interception of a beech forest in Northern Germany. *Agric Forest Meteorol* 1996;79:131–48.
- [31] Hutchings NJ, Milne R, Crowther JM. Canopy storage capacity and its vertical distribution in a Sitka spruce canopy. *J Hydrol* 1998;104:161–71.
- [32] Ishii H, Ford ED, Boscolo ME, Manriquez AC, Wilson ME, Hinckley TM. Variation in specific needle area of old-growth Douglas-fir in relation to needle age, within-crown position and epicormic shoot production. *Tree Physiol* 2002;22:31–40.
- [34] Keim RF, Skaugset AE. A linear system quantification of dynamic storage of precipitation on forest canopies. *Water Resour Res* 2004;40:W05208. doi:10.1029/2003WR002875.
- [35] Klaassen W, Bosveld F, de Water E. Water storage and evaporation as constituents of rainfall interception. *J Hydrol* 1998;212–213:36–50.
- [36] Laws JO. Measurements of the fall velocity of waterdrops and raindrops. *Trans Am Geophys Un* 1941;22:709–21.
- [37] Laws JO, Parsons DA. The relation of raindrop-size to intensity. *Trans Am Geophys Un* 1943;24:452–60.
- [38] Link TE, Unsworth M, Marks D. The dynamics of rainfall interception by a seasonal temperate rainforest. *Agric Forest Meteorol* 2004;124:171–91.

- [39] Linsley RK, Kolher MA, Paulhus JL. *Applied hydrology*. New York: McGraw-Hill; 1949.
- [40] Leyton L, Reynolds ERC, Thompson FB. Rainfall interception in forest and moorland. In: Sopper WE, Lull HW, editors. *Forest hydrology*. Oxford: Pergamon; 1967. p. 163–78.
- [41] Liu S. A new model for the prediction of rainfall interception in forest canopies. *Ecol Model* 1997;99:151–9.
- [42] Liu S. Estimation of rainfall storage capacity in the canopies of cypress wetlands and slash pine uplands in north-central Florida. *J Hydrol* 1998;207:32–41.
- [43] Llorens P, Gallart F. A simplified method for forest water storage capacity measurement. *J Hydrol* 2000;240:131–44.
- [44] Lundberg A. Evaporation of intercepted snow—review of existing and new measurement methods. *J Hydrol* 1993;151:267–90.
- [45] Mason BJ, Andrews JB. Drop-size distributions from various types of rain. *Quart J Roy Meteor Soc* 1960;86:346–53.
- [46] Merriam RA. A note on the interception loss equation. *J Geophys Res* 1960;65:3850–1.
- [47] Massman WJ. The derivation and validation of a new model for the interception of rainfall by forests. *Agric Meteorol* 1983;28:261–86.
- [48] Miller WP. A solenoid-operated, variable intensity rainfall simulator. *Soil Sci Soc Am J* 1987;51:832–4.
- [49] Mosley MP. The effect of a New Zealand beech forest canopy on the kinetic energy of water drops and on surface erosion. *Earth Surf Proc Landf* 1982;7:103–7.
- [50] Mulder JPM. Simulating interception loss using standard meteorological data. In: Hutchison BA, Hicks BB, editors. *The forest–atmosphere interaction*. Dordrecht, The Netherlands: D. Reidel; 1985. p. 177–96.
- [51] Nash JE, Sutcliffe JV. River flow forecasting through conceptual models, I, A discussion of principles. *J Hydrol* 1970;10:282–90.
- [52] Oszyzcka B, Crowther JM. The application of gamma-ray attenuation to the determination of canopy mass and canopy water storage. *J Hydrol* 1981;49:355–68.
- [53] Parker GG, Harmon ME, Lefsky MA, Chen JQ, Van Pelt R, Weis SB, et al. Three-dimensional structure of an old-growth *Pseudotsuga–Tsuga* canopy and its implications for radiation balance, microclimate, and gas exchange. *Ecosystems* 2004;7:440–53.
- [54] Pike LH, Rydell RA, Denison WC. A 400-year-old Douglas fir tree and its epiphytes: biomass, surface area, and their distributions. *Can J Forest Res* 1977;7:680–99.
- [55] Pitman JI. Rainfall interception by bracken in open habitats—relations between leaf area, canopy storage and drainage rate. *J Hydrol* 1989;105:317–34.
- [56] Pitman JI. Rainfall interception by bracken litter—relationship between biomass, storage and drainage rate. *J Hydrol* 1989;111:281–91.
- [57] Pojar J, MacKinnon A. *Plants of the Pacific Northwest Coast*. Redmond (WA, USA): Lone Pine; 1984.
- [58] Rutter AJ, Kershaw KA, Robins PC, Morton AJ. A predictive model of rainfall interception in forests, 1. Derivation of the model from observations in a plantation of Corsican pine. *Agric Meteorol* 1971;9:367–84.
- [60] Singh VP. *Hydrologic systems: vol. 1. Rainfall-runoff modeling*. Englewood Cliffs (NJ, USA): Prentice-Hall; 1988.
- [61] Storck P, Lettenmaier DP, Bolton SM. Measurement of snow interception and canopy effects on snow accumulation and melt in a mountainous maritime climate, Oregon, United States. *Water Resour Res* 2002;38:1223. doi:10.1029/2002WR001281.
- [62] Teklehaimanot Z, Jarvis PG. Direct measurement of evaporation of intercepted water from forest canopies. *J Appl Ecol* 1991;28:603–18.
- [63] Thomas SC, Winner WE. Leaf area index of an old-growth Douglas-fir forest estimated from direct structural measurements in the canopy. *Can J Forest Res* 2000;30:1922–30.
- [64] Torres R, Alexander LJ. Intensity-duration effects on drainage: column experiments at near-zero pressure head. *Water Resour Res* 2002;38:1240. doi:10.1029/2001WR001048.
- [65] Trimble Jr GR, Weitzman S. Effect of a hardwood canopy on rainfall intensities. *Trans Am Geophys Un* 1954;35:226–34.
- [67] Vis M. Interception, drop size distributions and rainfall kinetic energy in four Colombian forest ecosystems. *Earth Surf Proc Landf* 1986;11:591–603.
- [68] Whelan MJ, Anderson JM. Modelling spatial patterns of throughfall and interception loss in a Norway spruce (*Picea abies*) plantation at the plot scale. *J Hydrol* 1996;186:335–54.
- [69] Xiao Q, McPherson EG, Ustin SL, Grismer ME. A new approach to modeling tree rainfall interception. *J Geophys Res* 2000;105:29173–88.